Hadron Compositions in p+p and Au+Au Collisions at High Transverse Momenta at √sNN=200 GeV

Agakishiev, G.; ...; Planinić, Mirko; ...; Poljak, Nikola; ...; Zoulkarneeva, Y.

Identified Hadron Compositions in $p + p$ and Au + Au Collisions at High Transverse Momenta at $\sqrt{s_{NN}} = 200$ GeV

G. Agakishiev,[18] M. M. Aggarwal,[30] Z. Ahammed,[48] A. V. Alakhverdyants,[18] I. Alekseev,[16] J. Alford,[19] B. D. Anderson,[19] C. D. Anson,[28] D. Arkhipkin,[3] G. S. Averichev,[18] J. Balewski,[23] L. S. Barnby,[2] D. R. Beavis,[3] R. Bellwied,[44] M. J. Betancourt,[23] R. R. Betts,[8] A. Bhasin,[17] A. K. Bhati,[30] H. Bichsel,[50] J. Bielcik,[10] J. Bielcikova,[11] L. C. Bland,[3] I. G. Bordyuzhin,[16] W. Borowski,[41] J. Bouchet,[19] E. Braidot,[27] A. V. Brandin,[26] S. G. Brovko,[5] E. Bruna,[53] S. Bueltmann,[29] I. Bunzarov,[18] T. P. Burton,[3] X. Z. Cai,[40] H. Caines,[53] M. Calderón de la Barca Sánchez,[5] D. Cebra,[5] R. Cendejas,[6] M. C. Cervantes,[42] P. Chaloupka,[11] S. Chattopadhyay,[48] H. F. Chen,[38] J. H. Chen,[40] J. Y. Chen,[52] L. Chen,[52] J. Cheng,[45] M. Cherney,[9] A. Chikanian,[53] W. Christie,[3] P. Chung,[11] M. J. M. Codrington,[42] R. Corliss,[23] J. G. Cramer,[50] H. J. Crawford,[4] X. Cui,[38] A. Davila Leyva,[43] L. C. De Silva,[44] R. R. Debbe,[3] T. G. Dedovich,[18] J. Deng,[39] A. A. Derevschikov,[32] R. Derradi de Souza,[7] L. Didenko,[3] P. Djawotho,[42] X. Dong,[22] J. L. Drachenberg,[42] J. E. Draper,[5] C. M. Du,[21] J. C. Dunlop,[3] L. G. Efimov,[18] M. Elnimr,[51] J. Engelage,[4] G. Eppley,[36] M. Estienne,[41] L. Eun,[31] O. Evdokimov,[8] P. Fachini,[3] R. Fatemi,[20] J. Fedorisin,[18] R. G. Fersch,[20] P. Filip,[18] E. Finch,[53] V. Fine,[3] Y. Fisyak,[3] C. A. Gagliardi,[42] D. R. Gangadharan,[28] F. Geurts,[36] P. Ghosh,[48] Y. N. Gorbunov,[9] A. Gordon,[3] O. G. Grebenyuk,[22] D. Grosnick,[47] A. Gupta,[17] S. Gupta,[17] W. Guryn,[3] B. Haag,[5] O. Hajkova,[10] A. Hamed,[42] L-X. Han,[40] J. W. Harris,[53] J. P. Hays-Wehle,[23] S. Heppelmann,[31] A. Hirsch,[33] G. W. Hoffmann,[43] D. J. Hofman,[8] B. Huang,[38] H. Z. Huang,[6] T. J. Humanic,[28] L. Huo,[42] G. Igo,[6] W. W. Jacobs,[15] C. Jena,[13] J. Joseph,[19] E. G. Judd,[4] S. Kabana,[41] K. Kang,[45] J. Kapitan,[11] K. Kauder,[8] H. W. Ke,[52] D. Keane,[19] A. Kechechyan,[18] D. Kettler,[50] D. P. Kikola,[33] J. Kiryluk,[22] A. Kisiel,[49] V. Kizka,[18] S. R. Klein,[22] D. D. Koetke,[47] T. Kollegger,[12] J. Konzer,[33] I. Koralt,[29] L. Koroleva,[16] W. Korsch,[20] L. Kotchenda,[26] P. Kravtsov,[26] K. Krueger,[1] L. Kumar,[19] M. A. C. Lamont,[3] J. M. Landgraf,[3] S. LaPointe,[51] J. Lauret,[3] A. Lebedev,[3] R. Lednicky,[18] J. H. Lee,[3] W. Leight,[23] M. J. LeVine,[3] C. Li,[38] L. Li,[43] W. Li,[40] X. Li,[33] X. Li,[39] Y. Li,[45] Z. M. Li,[52] L. M. Lima,[37] M. A. Lisa,[28] F. Liu,[52] T. Ljubicic,[3] W. J. Llope,[36] R. S. Longacre,[3] Y. Lu,[38] E. V. Lukashov,[26] X. Luo,[38] G. L. Ma,[40] Y. G. Ma,[40] D. P. Mahapatra,[13] R. Majka,[53] O. I. Mall,[5] S. Margetis,[19] C. Markert,[43] H. Masui,[22] H. S. Matis,[22] D. McDonald,[36] T. S. McShane,[9] A. Meschanin,[32] R. Milner,[23] N. G. Minaev,[32] S. Mioduszewski,[42] M. K. Mitrovski,[3] Y. Mohammed,[42] B. Mohanty,[48] M. M. Mondal,[48] B. Morozov,[16] D. A. Morozov,[32] M. G. Munhoz,[37] M. K. Mustafa,[33] M. Naglis,[22] B. K. Nandi,[14] Md. Nasim,[48] T. K. Nayak,[48] L. V. Nogach,[32] S. B. Nurushev,[32] G. Odyniec,[22] A. Ogawa,[3] K. Oh,[34] A. Ohlson,[53] V. Okorokov,[26] E. W. Oldag,[43] R. A. N. Oliveira,[37] D. Olson,[22] M. Pachr,[10] B. S. Page,[15] S. K. Pal,[48] Y. Pandit,[19] Y. Panebratsev,[18] T. Pawlak,[49] H. Pei,[8] T. Peitzmann,[27] C. Perkins,[4] W. Peryt,[49] P. Pile,[3] M. Planinic,[54] J. Pluta,[49] D. Plyku,[29] N. Poljak,[54] J. Porter,[22] A. M. Poskanzer,[22] C. B. Powell,[22] D. Prindle,[50] C. Pruneau,[51] N. K. Pruthi,[30] P. R. Pujahari,[14] J. Putschke,[53] H. Qiu,[21] R. Raniwala,[35] S. Raniwala,[35] R. L. Ray,[43] R. Redwine,[23] R. Reed,[5] H. G. Ritter,[22] J. B. Roberts,[36] O. V. Rogachevskiy,[18] J. L. Romero,[5] L. Ruan,[3] J. Rusnak,[11] N. R. Sahoo,[48] I. Sakrejda,[22] S. Salur,[22] J. Sandweiss,[53] E. Sangaline,[5] A. Sarkar,[14] J. Schambach,[43] R. P. Scharenberg,[33] A. M. Schmah,[22] N. Schmitz,[24] T. R. Schuster,[12] J. Seele,[23] J. Seger,[9] I. Selyuzhenkov,[15] P. Seyboth,[24] N. Shah,[6] E. Shahaliev,[18] M. Shao,[38] M. Sharma,[51] S. S. Shi,[52] Q. Y. Shou,[40] E. P. Sichtermann,[22] F. Simon,[24] R. N. Singaraju,[48] M. J. Skoby,[33] N. Smirnov,[53] D. Solanki,[35] P. Sorensen,[3] U. G. deSouza,[37] H. M. Spinka,[1] B. Srivastava,[33] T. D. S. Stanislaus,[47] S. G. Steadman,[23] J. R. Stevens,[15] R. Stock,[12] M. Strikhanov,[26] B. Stringfellow,[33] A. A. P. Suaide,[37] M. C. Suarez,[8] M. Sumbera,[11] X. M. Sun,[22] Y. Sun,[38] Z. Sun,[21] B. Surrow,[23] D. N. Svirida,[16] T. J. M. Symons,[22] A. Szanto de Toledo,[37] J. Takahashi,[7] A. H. Tang,[3] Z. Tang,[38] L. H. Tarini,[51] T. Tarnowsky,[25] D. Thein,[43] J. H. Thomas,[22] J. Tian,[40] A. R. Timmins,[44] D. Tlusty,[11] M. Tokarev,[18] T. A. Trainor,[50] S. Trentalange,[6] R. E. Tribble,[42] P. Tribedy,[48] B. A. Trzeciak,[49] O. D. Tsai,[6] T. Ullrich,[3] D. G. Underwood,[1] G. Van Buren,[3] G. van Nieuwenhuizen,[23] J. A. Vanfossen, Jr.,[19] R. Varma,[14] G. M. S. Vasconcelos,[7] A. N. Vasiliev,[32] F. Videbæk,[3] Y. P. Viyogi,[48] S. Vokal,[18] S. A. Voloshin,[51] M. Wada,[43] M. Walker,[23] F. Wang,[33] G. Wang,[6] H. Wang,[25] J. S. Wang,[21] Q. Wang,[33] X. L. Wang,[38] Y. Wang,[45] G. Webb,[20] J. C. Webb,[3] G. D. Westfall,[25] C. Whitten, Jr.,[6,*] H. Wieman,[22] S. W. Wissink,[15] R. Witt,[46] W. Witzke,[20] Y. F. Wu,[52] Z. Xiao,[45] W. Xie,[33] H. Xu,[21] N. Xu,[22] Q. H. Xu,[39] W. Xu,[6] Y. Xu,[38] Z. Xu,[3] L. Xue,[40] Y. Yang,[21] Y. Yang,[52] P. Yepes,[36] K. Yip,[3] I-K. Yoo,[34] M. Zawisza,[49] H. Zbroszczyk,[49] W. Zhan,[21] J. B. Zhang,[52] S. Zhang,[40] W. M. Zhang,[19] X. P. Zhang,[45] Y. Zhang,[22] Z. P. Zhang,[38] F. Zhao,[6] J. Zhao,[40] C. Zhong,[40] X. Zhu,[45] Y. H. Zhu,[40] and Y. Zoulkarneeva[18]

(STAR Collaboration)

[1]*Argonne National Laboratory, Argonne, Illinois 60439, USA*

[2]University of Birmingham, Birmingham, United Kingdom
[3]Brookhaven National Laboratory, Upton, New York 11973, USA
[4]University of California, Berkeley, California 94720, USA
[5]University of California, Davis, California 95616, USA
[6]University of California, Los Angeles, California 90095, USA
[7]Universidade Estadual de Campinas, Sao Paulo, Brazil
[8]University of Illinois at Chicago, Chicago, Illinois 60607, USA
[9]Creighton University, Omaha, Nebraska 68178, USA
[10]Czech Technical University in Prague, FNSPE, Prague, 115 19, Czech Republic
[11]Nuclear Physics Institute AS CR, 250 68 Řež/Prague, Czech Republic
[12]University of Frankfurt, Frankfurt, Germany
[13]Institute of Physics, Bhubaneswar 751005, India
[14]Indian Institute of Technology, Mumbai, India
[15]Indiana University, Bloomington, Indiana 47408, USA
[16]Alikhanov Institute for Theoretical and Experimental Physics, Moscow, Russia
[17]University of Jammu, Jammu 180001, India
[18]Joint Institute for Nuclear Research, Dubna, 141 980, Russia
[19]Kent State University, Kent, Ohio 44242, USA
[20]University of Kentucky, Lexington, Kentucky, 40506-0055, USA
[21]Institute of Modern Physics, Lanzhou, China
[22]Lawrence Berkeley National Laboratory, Berkeley, California 94720, USA
[23]Massachusetts Institute of Technology, Cambridge, Massachusetts 02139-4307, USA
[24]Max-Planck-Institut für Physik, Munich, Germany
[25]Michigan State University, East Lansing, Michigan 48824, USA
[26]Moscow Engineering Physics Institute, Moscow Russia
[27]NIKHEF and Utrecht University, Amsterdam, The Netherlands
[28]The Ohio State University, Columbus, Ohio 43210, USA
[29]Old Dominion University, Norfolk, Virginia, 23529, USA
[30]Panjab University, Chandigarh 160014, India
[31]Pennsylvania State University, University Park, Pennsylvania 16802, USA
[32]Institute of High Energy Physics, Protvino, Russia
[33]Purdue University, West Lafayette, Indiana 47907, USA
[34]Pusan National University, Pusan, Republic of Korea
[35]University of Rajasthan, Jaipur 302004, India
[36]Rice University, Houston, Texas 77251, USA
[37]Universidade de Sao Paulo, Sao Paulo, Brazil
[38]University of Science & Technology of China, Hefei 230026, China
[39]Shandong University, Jinan, Shandong 250100, China
[40]Shanghai Institute of Applied Physics, Shanghai 201800, China
[41]SUBATECH, Nantes, France
[42]Texas A&M University, College Station, Texas 77843, USA
[43]University of Texas, Austin, Texas 78712, USA
[44]University of Houston, Houston, Texas, 77204, USA
[45]Tsinghua University, Beijing 100084, China
[46]United States Naval Academy, Annapolis, Maryland 21402, USA
[47]Valparaiso University, Valparaiso, Indiana 46383, USA
[48]Variable Energy Cyclotron Centre, Kolkata 700064, India
[49]Warsaw University of Technology, Warsaw, Poland
[50]University of Washington, Seattle, Washington 98195, USA
[51]Wayne State University, Detroit, Michigan 48201, USA
[52]Institute of Particle Physics, CCNU (HZNU), Wuhan 430079, China
[53]Yale University, New Haven, Connecticut 06520, USA
[54]University of Zagreb, Zagreb, HR-10002, Croatia

(Received 4 October 2011; published 14 February 2012)

We report transverse momentum ($p_T \leq 15$ GeV/c) spectra of $\pi^{\pm}$, $K^{\pm}$, p, $\bar{p}$, K^0_S, and ρ^0 at midrapidity in $p + p$ and Au + Au collisions at $\sqrt{s_{NN}} = 200$ GeV. Perturbative QCD calculations are consistent with $\pi^{\pm}$ spectra in $p + p$ collisions but do not reproduce K and $p(\bar{p})$ spectra. The observed decreasing antiparticle-to-particle ratios with increasing p_T provide experimental evidence for varying quark and gluon jet contributions to high-p_T hadron yields. The relative hadron abundances in Au + Au at

$p_T \gtrsim 8$ GeV/c are measured to be similar to the $p + p$ results, despite the expected Casimir effect for parton energy loss.

DOI: 10.1103/PhysRevLett.108.072302 PACS numbers: 25.75.Dw, 13.85.Ni

Quarks and gluons are the fundamental particles carrying color charge and participating in the strong interaction. High-energy partons are produced through hard processes in hadron-hadron collisions and, like all particles carrying color or electric charges, lose energy while traversing the hot and dense medium created in heavy ion collisions [1,2]. In all model calculations, the amount of parton energy loss is proportional to the color-charge Casimir factor (the relative coupling strength of gluon radiation from quarks or from gluons), and strongly depends on the medium traversed and on the parton mass [1,3,4]. This energy loss suppresses hadron spectra at high p_T in heavy ion collisions, an effect referred to as jet quenching and quantified by the nuclear modification factors (R_{AA}, the ratio of heavy ion collision spectra to $p + p$ collision spectra scaled by the number of underlying binary nucleon-nucleon inelastic collisions) [1,5,6].

The study of identified hadron spectra at high p_T in $p + p$ collisions also provides quantitative constraints on model calculations based on perturbative quantum chromodynamics (pQCD) [7]. In next-to-leading order (NLO) pQCD calculations, inclusive production of single hadrons is described by the convolution of parton distribution functions (PDFs), parton-parton interaction cross sections, and fragmentation functions (FFs). Specifically, the FFs [8–10] were primarily derived from elementary electron-positron collisions. The NLO pQCD framework has been verified with calculations successfully describing the spectra of inclusive charged hadrons, π^0, and jets [5,6,11] at RHIC. However, the flavor-separated quark and gluon FFs are not well constrained, especially for baryon production. To understand further the mechanisms of particle production in $p + p$ collisions and parton interactions with the medium in heavy ion collisions, it is necessary to provide more stringent constraints on the quark and gluon FFs by comparing theoretical calculations with experimental data in the same kinematics in $p + p$ collisions.

Measurements sensitive to the flavor of the initial hard scattered parton will provide further constraints and insights into the jet quenching mechanism [1,3,4,12–17]. An open question is whether the interaction of the hard partons with the medium alters the relative abundances of the identified-particle spectra (jet chemistry). Two examples of these interactions with the medium are enhanced parton splitting [12] and flavor changes of the initial parton (jet conversion) [13]. These processes are expected to modify the high-p_T identified-particle ratios in heavy ion versus $p + p$ collisions. The centrality dependence of antiproton and pion spectra in Au + Au collisions indicates that the suppression magnitude for antiprotons is similar to that for pions [14]. This is unexpected since antiproton production is dominated by gluon fragmentation, while pions have a comparable contribution from both gluon and quark jets [8]. The Casimir factor for gluons is 9/4 times that for quarks, which is expected to induce larger energy loss when gluons traverse the medium [4]. Naively, this would result in more suppressed antiproton spectra compared to pion spectra. A jet conversion mechanism, where a parton can change flavor or color charge after interaction with a medium, has been proposed whose calculations show a net quark to gluon jet conversion in this medium [15]. This leads to a better agreement with experimental data [15,16]. It is also predicted that the suppression pattern of kaons would differ significantly from that of pions due to the notable difference in relative abundance of strange quarks produced in jets versus the statistical expectations in a hot and dense medium [13]. Experimental measurements of identified hadrons at high p_T in $p + p$ collisions are required to more accurately determine the $p + p$ reference and to provide further constraints to the FFs. Together with the Au + Au measurements, it will help to understand the parton interactions with the medium.

In this Letter, we report $\pi^{\pm}$, $K^{\pm}$, $p(\bar{p})$, K^0_S, and ρ^0 p_T spectra at midrapidity ($|y| < 0.5$) up to 15 GeV/c in $p + p$ collisions at $\sqrt{s_{NN}} = 200$ GeV. The hadron spectra and particle ratios in $p + p$ collisions are compared to NLO pQCD calculations with various FFs. In addition, spectra of $K^{\pm} + p(\bar{p})$ (measured by $h^{\pm} - \pi^{\pm}$), K^0_S, and ρ^0 in the 12% most central Au + Au collisions are presented. R_{AA} are presented for $K^{\pm} + p(\bar{p})$, K^0_S, $\pi^+ + \pi^-$, and ρ^0.

A total of 21×10^6 12% most central Au + Au collisions used in this analysis were taken in 2004 at STAR [18]. The central trigger was based on an on-line cut of energy deposited in the zero-degree calorimeters. The $p + p$ data used for this analysis were taken in 2005. Experimental study of identified hadrons at high p_T in $p + p$ collisions was made possible by two technical advances: (1) using the STAR barrel electromagnetic calorimeter (BEMC) [19] as a trigger device for charged hadrons in $p + p$ collisions; and (2) improving the calibration and understanding of the ionization energy loss (dE/dx) of charged particles in the relativistic rise region in the time projection chamber (TPC) [20]. The minimum bias $p + p$ collision events were identified by the coincidence of two beam-beam counters [5]. On-line triggers, which utilized a minimum bias trigger and the energy deposited in either a single BEMC tower (high tower trigger, HT) or in a contiguous $\Delta\eta \times \Delta\phi = 1 \times 1$ rad region (jet patch trigger, JP) of the BEMC, were used for the $p + p$ collisions. A total of 5.6×10^6 JP events with transverse energy

$E_T > 6.4$ GeV were used for $\pi^{\pm}$, $K^{\pm}$, and $p(\bar{p})$ analyses. To reduce trigger biases, only away-side particles (at azimuthal angles 90°–270° from the JP trigger) were used in the analysis. Another 5.1×10^6 events with $E_T > 2.5$ GeV (HT1), and 3.4×10^6 events with $E_T > 3.6$ GeV (HT2) were used for $K^0_S \to \pi^+\pi^-$ and $\rho^0 \to \pi^+\pi^-$ reconstruction by requiring that one of the daughter pions trigger the high tower. The trigger enhancement factor in the range of 10–1000 [21] and bias have been determined by embedding PYTHIA events in the STAR geometry and selecting events that pass various detector thresholds present in real events. Consistencies of spectra from minimum bias data sets and between charged and neutral hadrons in the overlapping p_T range were utilized to check the trigger corrections.

The dE/dx measured in the TPC was used to identify $\pi^{\pm}$, $K^{\pm}$, and $p(\bar{p})$ at $3 < p_T < 15$ GeV/c at midrapidity [14,22,23]. The pion, kaon, and proton yields were extracted from a three-Gaussian fit to the inclusive positively or negatively charged particle dE/dx distributions at a given momentum. The recalibrated dE/dx in the TPC [21] enabled us to measure high-p_T kaons. $K^0_S \to \pi^+ + \pi^-$ decays were identified through the V0 topology [24]. The $\rho^0 \to \pi^+ + \pi^-$ yields were obtained using cocktail methods, after like-sign $\pi^+\pi^+$ and $\pi^-\pi^-$ pair invariant mass distribution backgrounds were subtracted from unlike-sign $\pi^+\pi^-$ pair distributions [25]. For the line shape of $\rho^0 \to \pi^+ + \pi^-$, the procedure and formula in [25] were used with the ρ^0 mass at 775 MeV and Breit-Wigner width 155 MeV [26]. The possible σ^0 particle [27] (mass at ≈ 600 MeV and Breit-Wigner width scanning from 100 to 500 MeV) was included in the cocktail fit as part of the systematic study on effect of other contributions on ρ^0 yields. This results in $\pm 20\%$ systematic error in ρ^0 yields and improves the χ^2 per degree of freedom (χ^2/NDF) up to a factor of 3 to be around unity. The fit with best χ^2/NDF was used to obtain the default ρ^0 yields, where the σ^0/ρ^0 ratio is about 25% independent of p_T. An additional systematic check was performed using the modified Soeding parametrization for a possible interference effect [28] on ρ^0 line shape. This results in larger χ^2/NDF and ρ^0 yields are within the stated systematic uncertainty.

Acceptance and efficiency corrections were studied by Monte Carlo GEANT simulations. Weak-decay feed-down contributions (e.g., $K^0_S \to \pi^+ + \pi^-$) are subtracted from the pion spectra [14]. Inclusive p and $\bar{p}$ production are presented, without hyperon feed-down subtraction [14]. In central Au + Au collisions, systematic errors for K^0_S yields are 4%–10% [29], and those for ρ^0 yields are 32%, dominated by signal reconstructions (20%) and cocktail fits (20%). The systematic errors from low to high p_T for $\pi^{\pm}$, $K^{\pm}$, p, and $\bar{p}$ in $p + p$ collisions include uncertainties in efficiency ($\approx 5\%$), dE/dx position and width (5%–70%), momentum distortion due to charge buildup in the TPC volume (0%–12%), the smearing of the measured spectra due to momentum resolution (0%–7%), and trigger correction factors (40%–10%). Systematic uncertainties for K^0_S and ρ^0 yields in $p + p$ collisions include uncertainties in trigger enhancement factors and biases ($< 20\%$), momentum resolution (1%–20%), efficiency (5%), and cocktail fits of ρ^0 yields (20%). The normalization uncertainties on the invariant yields and cross sections are 8% and 14% in $p + p$ collisions, respectively. The cancellation of the correlated systematic errors is taken into account for the particle ratios.

The invariant yields $d^2N/(2\pi p_T dp_T dy)$ of $\pi^{\pm}$, $K^{\pm}$, K^0_S, ρ^0, p, and $\bar{p}$ from $p + p$ collisions, and those of $K + p(\bar{p})$, K^0_S, and ρ^0 in central Au + Au collisions are shown in Fig. 1. In $p + p$ collisions, our measurements are consistent with those from minimum bias collisions within systematic errors in the overlapping p_T region [23]. The $K^{\pm}$ and K^0_S yields are consistent within statistical and systematic uncertainties, which verifies that the JP trigger condition for the $K^{\pm}$ measurement was correctly accounted for in the simulation. Also shown in Fig. 1 are the NLO calculations for $\pi^{\pm}$, $K^{\pm}$, p, and $\bar{p}$ spectra based on AKK [9] and DSS [10] FFs. Both calculations are consistent with the charged pion spectra in $p + p$ collisions, but deviate from the kaon and proton spectra.

In Fig. 2, particle ratios are shown as star symbols as a function of p_T from $p + p$ collisions. Our results are consistent with minimum bias results [23] in the overlapping p_T region and are extended to $p_T \approx 15$ GeV/c. We show for the first time that at this collision energy, π^-/π^+, $\bar{p}/p$, and K^-/K^+ ratios decrease with increasing p_T in $p + p$ collisions at midrapidity. This indicates relatively

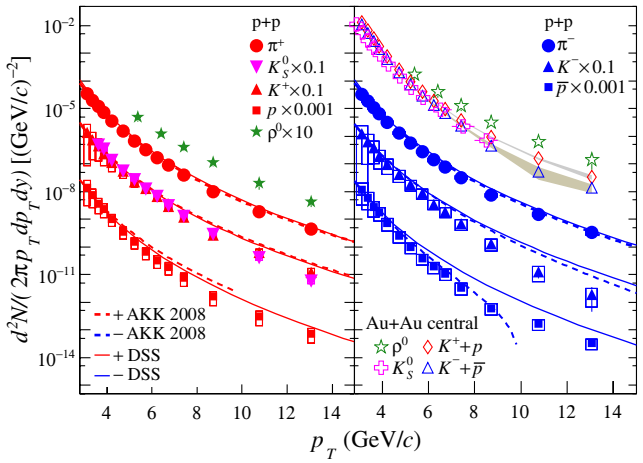

FIG. 1 (color online). The invariant yields $d^2N/(2\pi p_T dp_T dy)$ of $\pi^{\pm}$, $K^{\pm}$, K^0_S, ρ^0, p, and $\bar{p}$ from nonsingly diffractive $p + p$ collisions ($\sigma_{NSD} = 30.0 \pm 3.5$ mb [5]), those of $K + p(\bar{p})$, K^0_S, and ρ^0 in central Au + Au collisions, and NLO calculations with AKK [9] and DSS [10] FFs. The uncertainty of yields due to the scale dependence as evaluated in [10] is about a factor of 2. Bars and boxes (bands) represent statistical and systematic uncertainties, respectively.

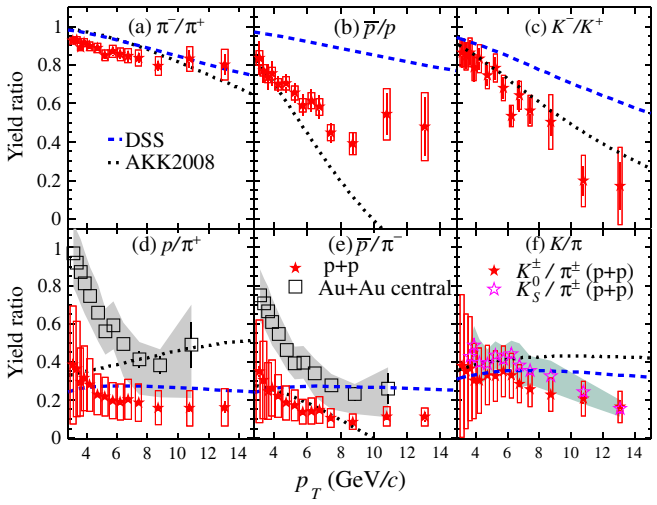

FIG. 2 (color online). Yield ratios π^-/π^+, $\bar{p}/p$, K^-/K^+, p/π^+, $\bar{p}/\pi^-$, and $(K^\pm, K^0_S)/\pi^\pm$ versus p_T in $p + p$ collisions, and nominal NLO calculations with AKK [9] and DSS [10] FFs without theoretical uncertainties. The open squares in panels (d) and (e) are the p/π^+ and $\bar{p}/\pi^-$ ratios in central Au + Au collisions [14] with updated uncertainties at high p_T, and all other data points are from $p + p$ collisions. Bars and boxes (bands) represent statistical and systematic uncertainties, respectively.

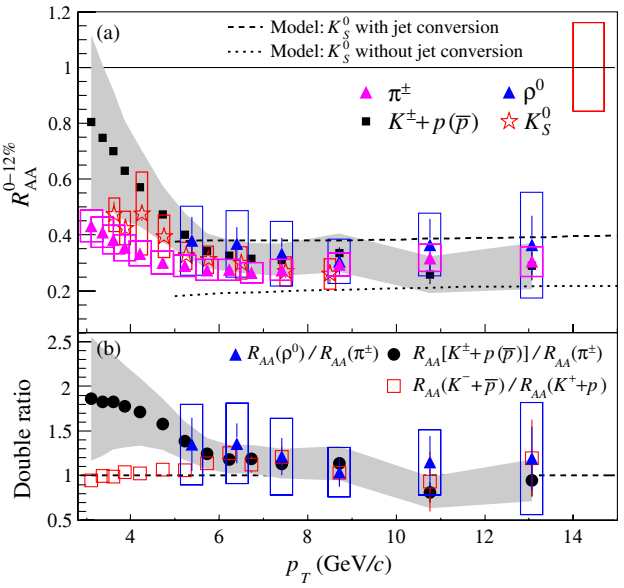

FIG. 3 (color online). (a) R_{AA} of $K^\pm + p(\bar{p})$, K^0_S, ρ^0, and $\pi^\pm$ in central Au + Au collisions as a function of p_T. The curves are the calculations for K^0_S R_{AA} with and without jet conversion in medium [15]. Bars and boxes (bands) represent statistical and systematic uncertainties, respectively. The height of the band at unity represents the normalization uncertainty. (b) The ratios of $R_{AA}[K^\pm + p(\bar{p}), \rho^0]$ to $R_{AA}(\pi^\pm)$ and $R_{AA}(K^- + \bar{p})$ to $R_{AA}(K^+ + p)$. The boxes and shaded bands represent the systematic uncertainties for $R_{AA}(\rho^0)/R_{AA}(\pi^\pm)$ and $R_{AA}[K^\pm + p(\bar{p})]/R_{AA}(\pi^\pm)$, respectively. The systematic uncertainties for $R_{AA}(K^- + \bar{p})/R_{AA}(K^+ + p)$ are 2%–12% and left off for clarity.

larger valence quark contributions to π^+, K^+, and p at high p_T than to their respective antiparticles. The NLO pQCD calculations with DSS and AKK FFs are consistent with the π^-/π^+ ratio but deviate from most of the other ratios measured. In the past, flavor-separated quark and gluon FFs were usually poorly determined for particles carrying a high fraction of the parton energy. Our measurements in $p + p$ collisions provide necessary constraints on the FFs in these ranges, which is crucial for the jet quenching studies at RHIC. Also shown in Fig. 2 are the p/π^+ and $\bar{p}/\pi^-$ ratios in central Au + Au collisions with central values same as in [14] and updated uncertainties at high p_T. For $p_T > 6$ GeV/c, the errors of p/π^+ and $\bar{p}/\pi^-$ in [14] were dominated by the systematic uncertainty from the dE/dx calibration, while the uncertainties from the kaon contamination were estimated to be insignificant with $K^-/K^+ = 0.94$ and K/π ratio in the range of 0.16 to 0.20. Although our current measurement of K/π ratio does not rule out this range of 0.16 to 0.20, we reevaluate the uncertainties in kaon contamination with the new measurements from $p + p$ collisions and update its error propagation to the p/π^+ and $\bar{p}/\pi^-$ ratios in central Au + Au collisions, shown in Fig. 2.

The nuclear modification factors R_{AA} and double ratios of R_{AA} are shown in Fig. 3 for $K^\pm + p(\bar{p})$, K^0_S, ρ^0, and $\pi^\pm$. Instead of using the individually extracted K and $p(\bar{p})$ yields [14] in the R_{AA}, we obtain the combined $K^\pm + p(\bar{p})$ yield with smaller systematic uncertainties by subtracting the charged pion yields from the inclusive hadron yields. At $p_T \gtrsim 8$ GeV/c, a common suppression pattern is observed for the different mesons (K^0_S, $\pi^\pm$, and ρ^0), despite the differences in quark flavor composition and mass. We also observe that $K^- + \bar{p}$ shows a magnitude of suppression similar to that of $K^+ + p$, despite the different contributions from gluon and quark jets and any Casimir factor effects on jet energy loss. A model for jet conversion in the hot and dense medium overpredicts the K^0_S enhancement at high p_T [13], as shown in Fig. 3.

It is worthwhile to highlight two important inputs to the jet conversion model calculation shown in Fig. 3: the kaon spectrum in $p + p$ collisions with the specific FF used in the model does not match our measurement, and the original $R_{AA}(K^0_S)$ in the absence of jet conversion was assumed to be equal to $R_{AA}(\pi^\pm)$ [13].

Enhanced parton splitting can also significantly change the jet hadron chemical composition [12]. In this model, heavier hadrons at high p_T become more abundant relative to the case without the enhanced parton splitting mechanism. Naively, the heavier ρ^0 meson is expected to be less suppressed than the $\pi^{\pm,0}$ and η [30] since all of them originate from the same parton fragmentation with similar constituent quark content. However, our measurements indicate that the ρ^0 and $\pi^\pm$ suppressions are similar in central Au + Au collisions. In addition, possible in-medium hadronization in the deconfined matter can lead

to less suppression for protons than for kaons and pions at $8 < p_T < 20$ GeV/c [31]. A comprehensive comparison requires quantitative modeling and calculations incorporating 3D hydrodynamics in an expanding medium [3,32] and proper light flavor-separated quark and gluon FFs. Since the protons are only a small part of the inclusive charged hadrons in $p + p$ collisions, we note that a factor of 2 enhancement of $R_{AA}(p + \bar{p})$ relative to $R_{AA}(\pi^{\pm})$ leads to a 20% enhancement of $R_{AA}[K^{\pm} + p(\bar{p})]$ compared to $R_{AA}(\pi^{\pm})$. This 20% enhancement falls within the range of our systematic uncertainties [23]. Improved identified-particle measurements in Au + Au collisions are needed to tighten constraints on phenomenological models related to jet quenching.

In summary, we report identified-particle p_T spectra at midrapidity up to 15 GeV/c from $p + p$ and Au + Au collisions at $\sqrt{s_{NN}} = 200$ GeV. The NLO pQCD models describe the $\pi^{\pm}$ spectra but fail to reproduce the K and $p(\bar{p})$ spectra at high p_T. The measured antiparticle to particle ratios are observed to decrease with increasing p_T. This reflects differences in scattering contributions to the production of particles and antiparticles at RHIC. At $p_T \gtrsim 8$ GeV/c, a common suppression pattern is observed for different particle species. Incorporating our $p + p$ data in generating the flavor-separated FFs in the same kinematic range will provide new inputs and insights into the mechanisms of jet quenching in heavy ion collisions.

We thank the RHIC Operations Group and RCF at BNL, the NERSC Center at LBNL and the Open Science Grid consortium for providing resources and support. This work was supported in part by the Offices of NP and HEP within the U.S. DOE Office of Science, the U.S. NSF, the Sloan Foundation, the DFG cluster of excellence "Origin and Structure of the Universe" of Germany, STFC of the United Kingdom, CNRS/IN2P3, FAPESP CNPq of Brazil, Ministry of Ed. and Sci. of the Russian Federation, NNSFC, CAS, MoST, and MoE of China, GA and MSMT of the Czech Republic, FOM and NWO of The Netherlands, DAE, DST, and CSIR of India, Polish Ministry of Sci. and Higher Ed., Korea Research Foundation, Ministry of Sci., Ed. and Sports of the Rep. of Croatia, and RosAtom of Russia.

*Deceased.

[1] M. Gyulassy *et al.*, arXiv:nucl-th/0302077; A. Kovner and U. A. Wiedemann, arXiv:hep-ph/0304151; in *Quark Gluon Plasma 3*, edited by R. C. Hwa and X. N. Wang (World Scientific, Singapore, 2004), pp. 123–248.
[2] J. Adams *et al.*, Nucl. Phys. **A757**, 102 (2005); I. Arsene *et al.*, Nucl. Phys. **A757**, 1 (2005); K. Adcox *et al.*, Nucl. Phys. **A757**, 184 (2005); B. B. Back *et al.*, Nucl. Phys. **A757**, 28 (2005).
[3] T. Renk and K. J. Eskola, Phys. Rev. C **76**, 027901 (2007).
[4] X. N. Wang, Phys. Rev. C **58**, 2321 (1998).
[5] J. Adams *et al.*, Phys. Rev. Lett. **91**, 172302 (2003).
[6] S. S. Adler *et al.*, Phys. Rev. Lett. **91**, 072301 (2003); S. S. Adler *et al.*, Phys. Rev. Lett. **91**, 241803 (2003); B. B. Back *et al.*, Phys. Lett. B **578**, 297 (2004); I. Arsene *et al.*, Phys. Rev. Lett. **91**, 072305 (2003).
[7] J. C. Collins and D. E. Soper, Annu. Rev. Nucl. Part. Sci. **37**, 383 (1987); J. C. Collins, D. E. Soper, and G. Sterman, Adv. Ser. Dir. High Energy Phys. **5**, 1 (1988).
[8] S. Albino, B. A. Kniehl, and G. Kramer, Nucl. Phys. **B725**, 181 (2005). The AKK FFs are the fragmentation functions with next-to-leading order perturbative QCD calculation. The program uses the light-flavor separated measurements of light charged hadron production in $e^+ + e^-$ collisions, thereby allowing the extraction of the flavor-dependent FFs of light quarks.
[9] S. Albino, B. A. Kniehl, G. Kramer, Nucl. Phys. **B803**, 42 (2008).
[10] W. Vogelsang (private communication); D. de Florian, R. Sassot, and M. Stratmann, Phys. Rev. D **76**, 074033 (2007). DSS FFs are the fragmentation functions from a global analysis with next-to-leading order perturbative QCD calculation. The data used in the fit include the available hadron spectra with flavor separation in $e^+ + e^-$, $e + p$, $p + p$, and $p + \bar{p}$ collisions.
[11] B. I. Abelev *et al.*, Phys. Rev. Lett. **97**, 252001 (2006).
[12] S. Sapeta and U. A. Wiedemann, Eur. Phys. J. C **55**, 293 (2008).
[13] W. Liu and R. J. Fries, Phys. Rev. C **77**, 054902 (2008).
[14] B. I. Abelev *et al.*, Phys. Rev. Lett. **97**, 152301 (2006); B. I. Abelev *et al.*, Phys. Lett. B **655**, 104 (2007); B. Mohanty *et al.*, J. Phys. G **35**, 104006 (2008); B. Mohanty *et al.*, arXiv:0705.0953.
[15] W. Liu, C. M. Ko, and B. W. Zhang, Phys. Rev. C **75**, 051901(R) (2007).
[16] X. Chen *et al.*, J. Phys. G **37**, 015004 (2010).
[17] P. Aurenche and B. G. Zakharov, Eur. Phys. J. C **71**, 1829 (2011).
[18] K. H. Ackermann *et al.*, Nucl. Instrum. Methods Phys. Res., Sect. A **499**, 624 (2003).
[19] M. Beddo *et al.*, Nucl. Instrum. Methods Phys. Res., Sect. A **499**, 725 (2003).
[20] M. Anderson *et al.*, Nucl. Instrum. Methods Phys. Res., Sect. A **499**, 659 (2003).
[21] Y. Xu *et al.*, Nucl. Instrum. Methods Phys. Res., Sect. A **614**, 28 (2010); H. Da *et al.*, arXiv:1112.2946; Y. Xu, Ph.D. thesis, USTC, 2009 [http://drupal.star.bnl.gov/STAR/theses/phd/yichunxu-0].
[22] M. Shao *et al.*, Nucl. Instrum. Methods Phys. Res., Sect. A **558**, 419 (2006).
[23] J. Adams *et al.*, Phys. Lett. B **637**, 161 (2006).
[24] B. I. Abelev *et al.*, Phys. Rev. C **75**, 064901 (2007).
[25] J. Adams *et al.*, Phys. Rev. Lett. **92**, 092301 (2004); B. I. Abelev *et al.*, Phys. Rev. C **78**, 044906 (2008).
[26] P. Fachini *et al.*, J. Phys. G **35**, 104063 (2008).
[27] R. Garcia-Martin *et al.*, Phys. Rev. Lett. **107**, 072001 (2011).
[28] B. I. Abelev *et al.*, Phys. Rev. C **77**, 034910 (2008).
[29] H. Agakishiev *et al.*, arXiv:1107.2955.
[30] S. S. Adler *et al.*, Phys. Rev. Lett. **96**, 202301 (2006).
[31] R. Bellwied and C. Markert, Phys. Lett. B **691**, 208 (2010).
[32] K. J. Eskola, H. Paukkunen, and C. A. Salgado, Nucl. Phys. **A830**, 599c (2009).